



Cite this: *Polym. Chem.*, 2022, **13**,
6377

Towards degradable polyethylene: end-functionalised polyethylene (PE-X) and PE-I/LDPE blends from iron-catalysed chain growth of ZnEt₂ with ethylene†

Richard von Goetze,^a Ahmad Aljaber,^a Koon-Yang Lee,^b  Gavin Hill,^b
Christopher Wallis^{a,b} and George J. P. Britovsek *^a

A series of end-functionalised polyethylene materials (PE-X) has been prepared *via* the catalysed chain growth (CCG) reaction of diethyl zinc with ethylene, catalysed by a bis(imino)pyridine iron catalyst activated by MAO. This CCG catalyst system enables the *in situ* formation of long alkyl chain zinc species Zn(PE)₂, which are subsequently quenched to form PE-X. Quenching with oxygen results in PE-OH, but the functionalisation appears to be limited to approximately 80% due to the formation of mixed [ZnR(OR)]_n clusters. Functionalisation with sulfur leads to polysulfides, PE-S_k-PE, whereby k is affected by temperature. Functionalisation with iodine leads to PE-I with high conversion, but the degree of functionalisation appears to be chain length dependant. PE-I has been blended with LDPE, either through solution mixing or *via* melt blending to give PE-I/LDPE blends with different chain lengths. Characterisation of the PE-I/LDPE blends has been carried by IR spectroscopy and thermal analysis (DSC). Surface analysis by FIB-SEM and EDX analysis up to 6 μm into the surface has shown a uniform distribution of PE-I within the LDPE matrix. The propensity of alkyl iodides to undergo photolytic cleavage makes these PE-I/LDPE materials interesting candidates for degradable PE.

Received 30th August 2022,
Accepted 27th October 2022

DOI: 10.1039/d2py01123a

rsc.li/polymers

Introduction

Polyethylene (PE) is currently the most widely used synthetic polymer on the market and accounts for almost one third of the total global plastics production, which translates to approximately 90 Mt per annum.^{1–3} A wide range of different types of PE are available, all with polymer properties designed for specific applications. Many of these properties cannot easily be obtained by other polymers at a reasonable cost, including polymers from bio-derived or renewable resources. The unique and tuneable properties of PE-based materials and their versatility, combined with their low cost and ease of production, have made PE the most successful polymer on the

market and the material of choice for many applications today and for some time to come.

The main classes of polyethylene, LDPE, LLDPE, HDPE and UHMWPE, are prepared using different catalyst systems and, in the case of LLDPE through incorporation of co-monomers.⁴ Post-functionalisation of polyethylene can be carried out to modify certain polymer properties using a range of methods,⁵ for example through oxidation or chlorination of surface C–H bonds to prepare oxygenated or chlorinated PE.⁶ An alternative strategy to introduce specific functionality into polyolefins like PE is through melt-blending with end-functionalised polyethylene. In this context, well-defined functionalised polymers, so called smart materials, have become increasingly important targets in recent years.^{7–10}

Commercially available end-functionalised alkanes are only up to C₁₈. A convenient method to generate longer polyethylene chains with reactive chain ends (PE-X) is *via* reversible coordinative chain transfer polymerisation.^{9,11} This method uses a polymerisation catalyst (M¹) in combination with a chain transfer agent (M²) and makes use of a very fast and reversible exchange of the growing polymer chains (P¹ and P²) between the catalyst and a transfer agent (see eqn. (1)). A range of transition metal catalysts can be used, whereby transfer

^aDepartment of Chemistry, Imperial College London, MSRH, 82 Wood Lane, White City Campus, London W12 0BZ, UK. E-mail: g.britovsek@imperial.ac.uk

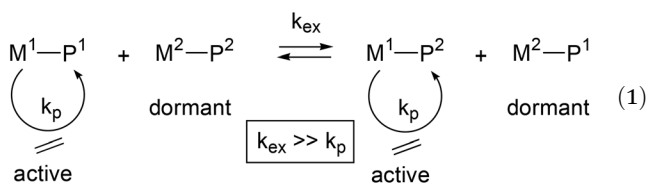
^bPolymateria Ltd, Innovation-Hub, 80 Wood Lane, London, W12 0BZ, UK

^cDepartment of Aeronautics, Imperial College London, Exhibition Road, South Kensington Campus, London SW7 2AZ, UK

† Electronic supplementary information (ESI) available: Materials and methods, synthetic procedures, NMR, details for DSC and SEM analysis. See DOI: <https://doi.org/10.1039/d2py01123a>

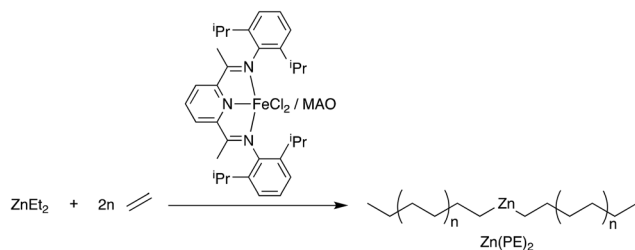


agents are typically based on main group metals such as trialkyl aluminium,^{12–23} dialkyl magnesium,^{24–27} or dialkyl zinc reagents.^{12,28–33}

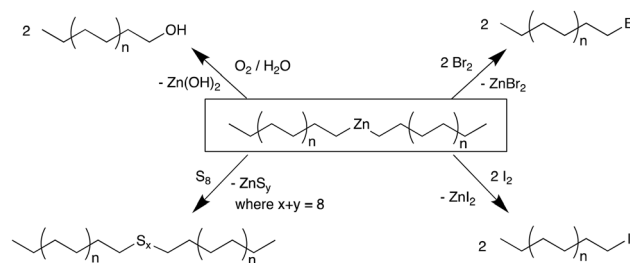


A specific case where all metal alkyl chains are equally engaged in reversible coordinative chain transfer polymerisation is termed *Catalysed Chain Growth* (CCG).²⁸ CCG leads to a controlled growth of all alkyl chains on the main group metal (M^2) and results in $M(PE)_n$ with a Poisson distribution of PE chain lengths.³⁴ Cleavage of the $M-C$ bond in $M(PE)_n$ can be achieved in a number of ways. Hydrolysis (or protonolysis with HX) will generate linear alkanes $PE-H$ and $Zn(OH)_2$ (or ZnX_2), whereas the use of an additional catalyst that enables a fast termination *via* β -H transfer can generate a Poisson distribution of linear 1-alkenes.^{12,35} The high reactivity of main group $M-C$ bonds can also be exploited to generate end-functionalised polyethylenes $PE-X$, where X is for example a halide, hydroxide or amine functionality. End-functionalised $PE-X$ can then be used for the preparation of diblock copolymers.^{8,22,36–41} Oxidative workup of the $M-C$ bonds to generate $PE-OH$ has been reported for aluminium,^{21,23,42} magnesium,^{43,44} and zinc alkyls.^{36–41,45,46} The end-functionalisation of polyethylene using magnesium alkyls as the chain transfer agent in combination with a neodymium polymerisation catalyst $[(C_5Me_5)_2NdCl_2Li(OEt_2)_2]$, first reported by Mortreux,²⁴ has been extensively investigated by Boisson and D'Agosto and co-workers. In these CCG reactions, $Mg(PE)_2$ is used to generate various end-functionalised $PE-X$.^{43,44,47–50}

Here we report our studies on the iron-based CCG reaction using $ZnEt_2$ to prepare $Zn(PE)_2$ with defined chain lengths and conversion to a range of end-functionalised $PE-X$ materials. While the reactivity of $Zn(PE)_2$ in many ways resembles that of $Mg(PE)_2$, key advantages of the Fe/Zn system are the ease of synthesis and handling of the iron-based catalyst, the use of highly abundant and cheap first row metals iron and zinc, and crucially, the absence of any alkene by-products, which is often seen in other systems. A range of functionalised $PE-X$ materials has been prepared in this study, where X is either



Scheme 1 Catalysed chain growth of $ZnEt_2$ using the catalyst system $[(2,6\text{-diacetylpyridinebis}(2,6\text{-diisopropylanil}))FeCl_2]$ (**1**) and MAO.



Scheme 2 Overview of reactions of $Zn(PE)_2$ with Group 16 and 17 elements.

from Group 16 ($PE-OH$ and $PE-S_k-PE$, where $k = 1-8$) or Group 17 ($PE-I$, $PE-Br$) (see Scheme 2).

A further aim in this work has been the preparation of polymer blends between $PE-I$ and LDPE. Such blends could improve the degradability of polyethylene because alkyl iodides are prone to homolysis of the $C-I$ bond under UV irradiation,^{51–53} generating alkyl radicals which in the presence of air can form alkyl peroxy radicals,⁵⁴ and these alkylperoxy radicals are key intermediates in the degradation of polyethylene.⁵⁵ Furthermore, the low entanglement molecular weight for polyethylene of $M_e \sim 1250 \text{ g mol}^{-1}$,⁵⁶ suggests chain lengths of approximately 90 carbons will be sufficient to ensure efficient entanglement of $PE-I$ within the polyethylene matrix and avoid any leaching of the $PE-I$ additive.

Results and discussion

Synthesis and characterisation of $Zn(PE)_2$

The preparation of $Zn(PE)_2$ was carried out using our previously described method from $ZnEt_2$ and $[(2,6\text{-diacetylpyridinebis}(2,6\text{-diisopropylanil}))FeCl_2]$ (**1**) in combination with MAO as the activator, as shown in Scheme 1.²⁸ The extremely fast alkyl exchange reaction between iron and zinc ensures the formation of $Zn(PE)_2$ with excellent selectivity and low dispersity. By varying the reaction time and the ratio between $Zn(Et)_2$ and **1**, the chain length of the resulting PE chains can be controlled (see Table 1). Upon hydrolysis, a Poisson distribution of alkanes is obtained with a low dispersity of molecular weights.²⁸

In the absence of the chain transfer agent $ZnEt_2$, the catalyst system **1**/MAO polymerises ethylene with very high activity and produces high molecular weight polyethylene (run 1 in Table 1).⁵⁷ Small amounts of $ZnEt_2$ (<250 equiv., run 2) have little effect on the polymerisation reactions and only at Zn/Fe ratios of >300 equiv., catalysed chain growth to form $Zn(PE)_2$ is observed. While larger Zn/Fe ratios will produce more $Zn(PE)_2$, this results in shorter chains within a given time and also lowers the catalytic activity, probably due to competitive binding of $ZnEt_2$ *versus* ethylene to the catalyst.⁵⁸ $Zn(PE)_2$ can be isolated from the reaction mixture by filtration and characterised by NMR and IR spectroscopy (see Fig. S1–3†). The characteristic triplet for the $ZnCH_2$ moiety is found at



Table 1 Chain length variations in Zn(PE)₂ at different Zn/Fe ratios

| Run | ZnEt ₂ [mmol] | ZnEt ₂ Equiv. | Activity [g mmol ⁻¹ h bar ⁻¹] | λ ^a | C _n ^b |
|-----|--------------------------|--------------------------|--|----------------|-----------------------------|
| 1 | 0 | 0 | PE ^c | — | — |
| 2 | 2.5 | 250 | PE ^c | — | — |
| 3 | 3.0 | 300 | 1380 | 31 | 64 |
| 4 | 3.5 | 350 | 1420 | 21 | 44 |
| 5 | 4.0 | 400 | 820 | 14 | 30 |
| 6 | 4.5 | 450 | 600 | 11 | 24 |
| 7 | 5.0 | 500 | 690 | 8 | 18 |
| 8 | 5.5 | 550 | 482 | 7 | 16 |
| 9 | 6.0 | 600 | 500 | 4 | 10 |

Conditions: catalyst **1** (10 μmol), MAO (100 eq.), toluene solvent (30 mL), room temperature, 1 barg ethylene, 1 hour reaction time. ^a λ = mean number of ethylene units inserted, determined by GC analysis. ^b C_n = mean chain length, determined by ¹³C-NMR analysis. ^c No exchange to zinc is observed.

0.30 ppm in the ¹H NMR and at 16.3 ppm in the ¹³C NMR spectrum, as well as the in-plane rocking vibration at 628 cm⁻¹, typical for ZnCH₂ units.⁵⁹ The high reactivity of the Zn–C bond can be exploited to prepare a range of end-functionalised PE-X compounds, as illustrated in Scheme 2

Hydrolysis of Zn(PE)₂ results in a distribution of linear alkanes. The Poisson distribution of the *n*-alkane oligomers allows quantitative ¹³C NMR analysis to be used to estimate the mean chain length C_n by comparing integrals for CH₃ with those for CH₂ signals (Table 1, last column). Further analysis can be achieved by GC-FID. The average molecular weight is generally too low for accurate GPC analysis, whereas analysis by GC-FID will only capture part of the total distribution, because the longer alkanes are only partially soluble and insufficiently volatile for GC analysis, as illustrated in Fig. 1. Only the first part of the total distribution is therefore quantifiable, and these values can be used as inputs for the Poisson equation (eqn. (2)) to extract λ, the mean number of inserted ethylene units (*L* is the amount of catalyst used). The total amount of each alkane of chain length *n* obtained at the end of the reaction can then be calculated.^{60,61} For example, the calculated value of λ = 14 for run 5 in Table 1 suggests an average chain length of 30 carbons which is very close to the value of 30 carbons determined by ¹³C NMR spectroscopy (see Table 1 for other values). Comparison of the average chain lengths determined by GC and NMR analysis shows excellent agreement (Fig. 2). This fitting method allows the entire product distribution to be determined from a subset of experimental data obtained by GC analysis.

$$\text{Poisson equation : } \text{mol}(n)_{\text{tend}} = \frac{L\lambda^n}{n!} e^{-\lambda} \quad (2)$$

There appears to be no convenient nomenclature to describe mixtures of compounds with long alkyl chains, where the length of the chains follows a Poisson distribution, other than quoting an M_n value. In order to describe the chain length in our product mixtures, we will henceforth use the italicised *n* value (*n*) to describe an average chain length, *i.e.*

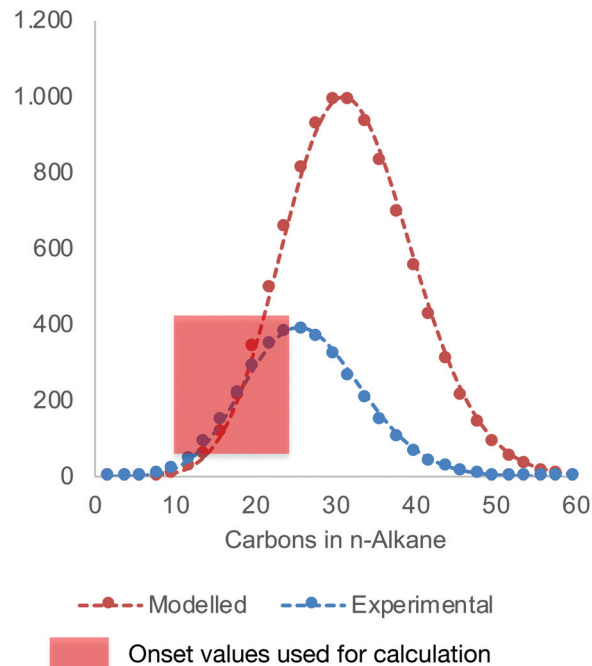


Fig. 1 Experimentally determined *n*-alkane distribution by GC-FID (blue) versus calculated distribution based on the Poisson equation (red, data from run 5 in Table 2).

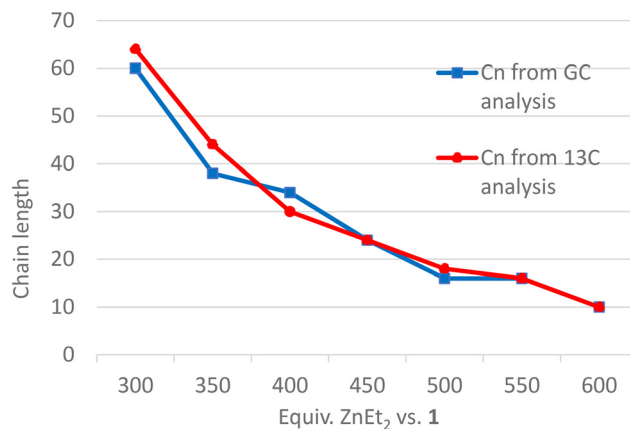


Fig. 2 Zn(PE)₂ chain length (C_n) as a function of Zn/Fe ratio.

C_nH_{2n±2} to describe a mixture of alkanes with an average chain length *n*. We will use the same nomenclature for other related compounds, *i.e.* Zn(C₃₀H₆₁)₂ will result in C₃₀H₆₂ upon hydrolysis, or C₃₀H₆₁I upon reaction with iodine. C₃₀H₆₁I is thus a mixture of alkyl iodides with chain lengths clustered around C₃₀, whereas C₃₀H₆₁I would be the pure compound.

End-functionalisation with oxygen

Initial experiments with dipentylzinc as a model compound for Zn(PE)₂ and synthetic air (80% N₂/20% O₂, dry) resulted in a mixed alkyl alkoxide complex, [Zn(OPent)Pent]_n, according to NMR analysis (see Fig. S4 and 5[†]), presumably a tetramer (*n* = 4) as seen in related examples.^{62,63} Hydrolysis of the zinc



cluster resulted in pentanol with 78% selectivity, the remainder being pentane. A reaction with pure oxygen instead of air gave similar results but was subsequently avoided for safety reasons. Subsequently, CCG reactions using ZnEt_2 and catalyst **1** ($\text{Zn}/\text{Fe} = 300$) have been carried out at 1 bar ethylene pressure and the product $\text{Zn}(\text{PE})_2$ was reacted with air prior to hydrolysis (see Table 2). Reactions were carried out using different amounts of catalyst, which did affect the activity somewhat. The products in both reactions have a similar average chain length, analysed as $\text{C}_{68}\text{H}_{137}\text{OH}$ according to ^{13}C NMR with 65–74% OH-functionalisation, the remainder of the product mixture being linear alkanes.

The formation of end-functionalised PE-OH from the reaction of $\text{Zn}(\text{PE})_2$ with oxygen has been investigated previously using Ziegler–Natta catalysts and metallocenes,^{45,46,64} titanium guanidate catalysts,⁴¹ and also with the Fe/Zn catalyst system use here.^{36–40} In all these reports, the degree of OH-functionalisation is less than 80%, with the remainder being alkanes (PE-H) formed upon hydrolysis. The incomplete reaction of zinc alkyls with oxygen is likely due to the formation of mixed zinc alkyl alkoxide “ $\text{ZnR}(\text{OR})$ ” clusters, as reported by Lewinski.^{62,65,66} For example, the reaction of ZnMe_2 with oxygen has been reported to generate $[\text{Zn}(\text{OMe})_2(\text{Zn}(\text{OMe})\text{Me})_6]$, which upon hydrolysis would only yield 57% MeOH. It is possible that for ZnR_2 with longer alkyl chains, similar $[\text{Zn}(\text{OR})_x\text{R}_y]$ clusters are generated which upon hydrolysis will generate different yields of ROH.^{62,67,68} We can thus conclude that end-functionalisation of $\text{Zn}(\text{PE})_2$ to generate PE-OH appears to have an upper limit of approximately 80% selectivity, because this functionalisation suffers from an inherent problem due to the formation of stable mixed alkyl/alkoxide zinc clusters upon reaction with oxygen.

End-functionalisation with sulfur

The incorporation of sulfur into polymers, for example the vulcanisation of rubber, has been an important aspect in polymer chemistry for a long time, and is currently finding renewed interest for other polymers.^{69–71} The reaction of main group alkyls with elemental sulfur has been known for some time and generally results in the formation of dialkyl polysulfides $\text{R-S}_k\text{-R}$.⁷² Boisson *et al.* have shown that $\text{Mg}(\text{PE})_2$ reacts with sulfur to generate PE- S_k -PE polysulfide polymers, where $k =$

1–8. Previous studies on the reaction between ZnEt_2 with sulfur in equimolar amounts resulted in the formation of $[\text{Zn}(\text{SEt})\text{Et}]_n$ clusters such as $[\text{Zn}(\text{SEt})\text{Et}]_{10}$,⁷³ similar as for the reaction with oxygen discussed in the previous section. Increasing the ratio of sulfur to zinc leads to the formation of $[(\text{ZnS})\text{Zn}(\text{SEt})_2]_n$ clusters, together with the formation of SEt_2 and S_2Et_2 .⁷⁴

Initial reactions of dipentylzinc with sulfur in an equimolar ratio showed the formation of $\text{C}_5\text{H}_{11}\text{-S}_k\text{-C}_5\text{H}_{11}$ (where the ratio of $k = 1 : 2 : 3 +$ was 21 : 42 : 37), together with unreacted dipentylzinc (see Fig. S6†). The reaction of excess sulfur (4 equiv.) with $\text{Zn}(\text{PE})_2$ resulted in the formation of PE- S_k -PE polymers with 71% functionalisation, the remainder being linear alkanes formed upon hydrolysis. Analysis by ^1H NMR reveals a ratio between PE-S-PE, PE-S₂-PE and PE-S₃₊-PE of 11 : 42 : 47 (see Fig. 3). Considering an average chain length of C_{22} in this case, an average value of $k = 4$ could be calculated from elemental analysis (see Table S1†). Analysis of PE- S_k -PE by Raman spectroscopy (Fig. S8†) has shown a characteristic C–S vibration at 744 cm^{-1} .⁷⁵ When PE- S_k -PE was heated in toluene at 80 °C for one hour a reduction of k was observed, specifically in the amount of PE- S_k -PE with $k \geq 3$ (see Fig. S7†), in line with the general thermal instability of polysulfides with $k > 3$.⁷⁶

End-functionalisation with iodine and bromine

The reaction of $\text{Zn}(\text{PE})_2$ with an excess I_2 results in 1-iodoalkanes (PE-I), together with ZnI_2 . A range of 1-iodoalkanes with various average chain lengths has been prepared, a selection is shown in Table 3. The products have been analysed by GC, ^1H , ^{13}C NMR and IR spectroscopy, as well as thermal analysis (Fig. S10–15†). Analysis of long chain 1-iodoalkanes by GC is reliable for short chain lengths up to C_{20} and fitting of the GC results to the Poisson formula allows full characterisation of the distribution of chain lengths to be determined (see Fig. S14†). Average chain length values have been determined by ^{13}C NMR analysis (see Fig. S11†). IR spectroscopic analysis can also be used for relatively short alkyl iodides, using the ratio of $\nu(\text{C-H})$ signal at 3000 cm^{-1} relative to the characteristic $\nu(\text{C-I})$ stretch at 603 cm^{-1} (see Fig. S15–17†).

Thermal analysis was carried out on a series of four longer chain PE-I samples with different chain lengths, ranging from C_{48} to C_{88} alkyl iodides. Analysis by DSC shows two endothermic processes (Fig. 4), one centred around 60–70 °C and another around 110–120 °C. The former signal is more dominant for the shorter chain alkyl iodides, whereas the latter becomes the main transition for the longer chain products. Melting points for linear alkyl iodides $\text{C}_n\text{H}_{2n+1}\text{I}$ of different chain lengths follow a hyperbolic relationship (Fig. S20†), approaching the melting point of HDPE for $n \rightarrow \infty$, and the melting points of pure $\text{C}_{48}\text{H}_{97}\text{I}$ and $\text{C}_{88}\text{H}_{177}\text{I}$ are 91 °C and 110 °C, respectively.^{77,78} The two transitions seen here are due to the fact that we have mixtures of linear alkyl iodides with different chain lengths that lead to the formation of solid solutions before complete melting of the material takes place. Similar complex behaviour has been reported for mixtures of alkanes and perfluorinated alkanes.^{79,80}

Table 2 Synthesis of PE-OH from $\text{Zn}(\text{PE})_2$ upon reaction with air

| Run | Yield [g] | Zn/Fe ratio | Activity [$\text{g mmol}^{-1}\text{ h bar}^{-1}$] | λ^c | C_n^d | Funct.(%) |
|----------------|-----------|-------------|---|-------------|----------------|-----------|
| 1 ^a | 3.84 | 300 | 384 | 33 | 68 | 74 |
| 2 ^b | 19.9 | 300 | 497 | 33 | 68 | 65 |

^a Conditions: catalyst **1** (10 μmol), MAO (100 eq.), toluene solvent (30 mL), room temperature, 1 bar ethylene, 1 hour reaction time, quenched with air ^b Conditions: catalyst **1** (40 μmol), MAO (100 eq.), toluene solvent (120 mL), room temperature, 1 bar ethylene, 1 hour reaction time, quenched with air ^c λ = mean number of ethylene units inserted, determined by GC analysis ^d C_n = mean chain length, determined by quantitative ^{13}C -NMR analysis



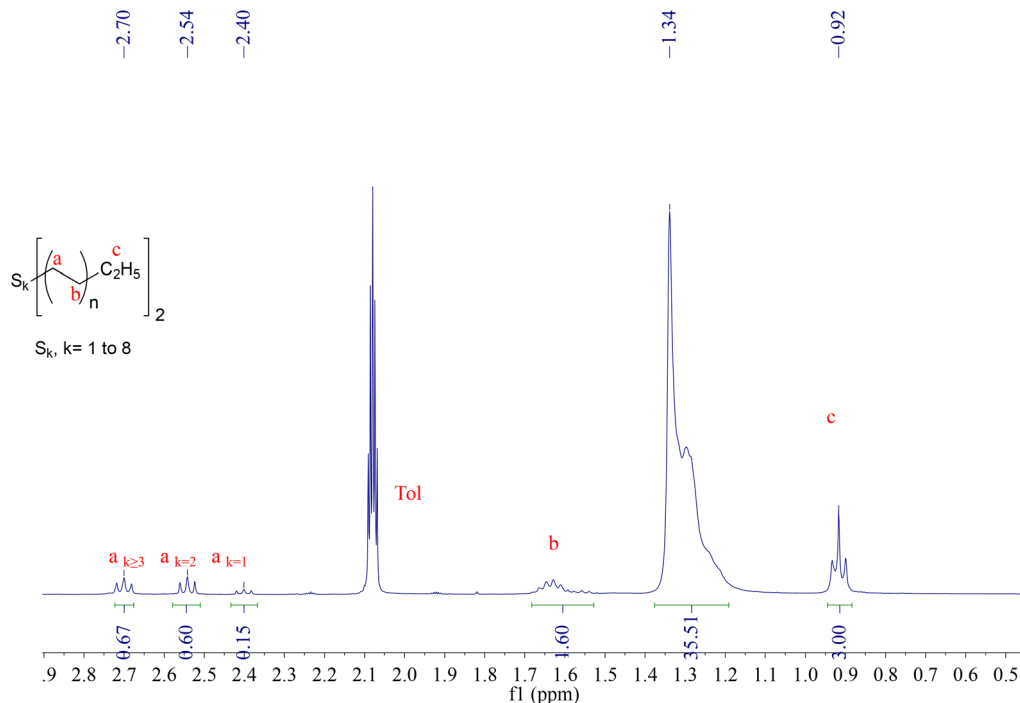


Fig. 3 ^1H -NMR spectrum in d_8 -toluene at 298K of $\text{PE-S}_k\text{-PE}$ ($k = 1-8$) obtained from the reaction of $\text{Zn}(\text{PE})_2$ with 4 equiv. sulfur. $\text{Zn}(\text{PE})_2 = \text{Zn}(\text{C}_{22}\text{H}_{45})_2$ in this case.

Table 3 Synthesis of PE-I from $\text{Zn}(\text{PE})_2$ with various chain lengths

| Run | Eq. Zn | Activity [g mmol $^{-1}$ h bar $^{-1}$] | Chain length a (C_n) | PE-I b (%) |
|-----|--------|---|--------------------------------|---------------|
| 1 | 300 | 1460 | 70 | 89 |
| 2 | 350 | 1220 | 46 | 96 |
| 3 | 450 | 950 | 40 | 97 |
| 4 | 500 | 900 | 30 | 98 |
| 5 | 650 | 640 | 12 | 100 |

Conditions for the polymerization reactions: catalyst **1** (10 μmol), MAO (100 eq.), toluene solvent (50 mL), 30 $^\circ\text{C}$, 1 barg ethylene, 1 hour reaction time. $^a C_n$ = average chain length, determined by ^{13}C NMR analysis. b Iodo-functionality yield determined by ^1H NMR analysis.

Whilst selectivities for the formation of PE-I are typically very high (>90%), the functionalisation appears to depend to some degree on the alkyl chain length, something that was also noted by Boisson in catalysed chain growth reactions of magnesium alkyls followed by iodine quenching.⁴⁸ For example, the degree of functionalisation is quantitative for $\text{C}_{20}\text{H}_{41}\text{I}$, but decreases to 97% for $\text{C}_{30}\text{H}_{61}\text{I}$ and 89% for $\text{C}_{70}\text{H}_{141}\text{I}$, the remainder being the corresponding alkanes (see Fig. S12 \dagger). This may be due to the reduced solubility of $\text{Zn}(\text{PE})_2$ with increasing chain length, or alternatively, encapsulation of the reactive zinc centres with increased PE chain length could result in restricted access to the metal centre and reduced reactivity with I_2 . Unreacted zinc-carbon bonds are eventually cleaved upon hydrolysis, resulting in the formation of alkanes.

Analogous to the reaction of $\text{Zn}(\text{PE})_2$ with iodine, reactions with bromine result in the formation of PE-Br. Upon addition of

Br_2 to a solution of $\text{Zn}(\text{PE})_2$ in toluene, $\text{C}_{32}\text{H}_{65}\text{Br}$ was obtained with 67% functionalisation, the remainder being $\text{C}_{32}\text{H}_{66}$ (see Fig. S18 and 19 \dagger). The reason for the lower functionalisation is not clear at this stage, but it should be noted that compared to iodine, the addition of bromine is considerably more reactive and may have led to some decomposition of alkyl zinc species.

Synthesis and characterisation of PE-I/LDPE polymer blends

A series of polymer blends has been prepared by incorporating PE-I into LDPE (SABIC N0W2021). The polymer blends were prepared by two different methods, either by solution mixing or melt blending. Solution mixing involved dissolving LDPE in hot toluene,⁸¹ followed by the addition of PE-I and precipitation of the resulting PE-I/LDPE polymer blend in methanol. Melt blending of PE-I and LDPE was carried out *via* co-extrusion at 130 $^\circ\text{C}$ (see ESI \dagger). TGA analysis has shown that PE-I and LDPE are thermally stable up to 200 $^\circ\text{C}$ (Fig. S21 \dagger). LDPE was blended with $\text{C}_{18}\text{H}_{37}\text{I}$, $\text{C}_{30}\text{H}_{61}\text{I}$ and $\text{C}_{70}\text{H}_{141}\text{I}$ at 10 wt% loading. Analysis of the polymer blends was carried out by IR spectroscopy based on the characteristic signals at 1163 cm^{-1} for $\omega(\text{CH}_2\text{I})$ and 603 cm^{-1} for $\nu(\text{C-I})$ (see Fig. S15 \dagger). Despite dilution in the LDPE matrix the characteristic IR signals can be clearly observed (Fig. 5 for solution mixing and S22 \dagger for melt blending). Further characterisation was carried out by DSC analysis, which shows superposition of the DSC profiles for LDPE and PE-I (Fig. S23 \dagger).

In order to establish the dispersion of PE-I throughout the PE-I/LDPE polymer blend, surface analysis has been carried out on the material obtained through solution blending, using



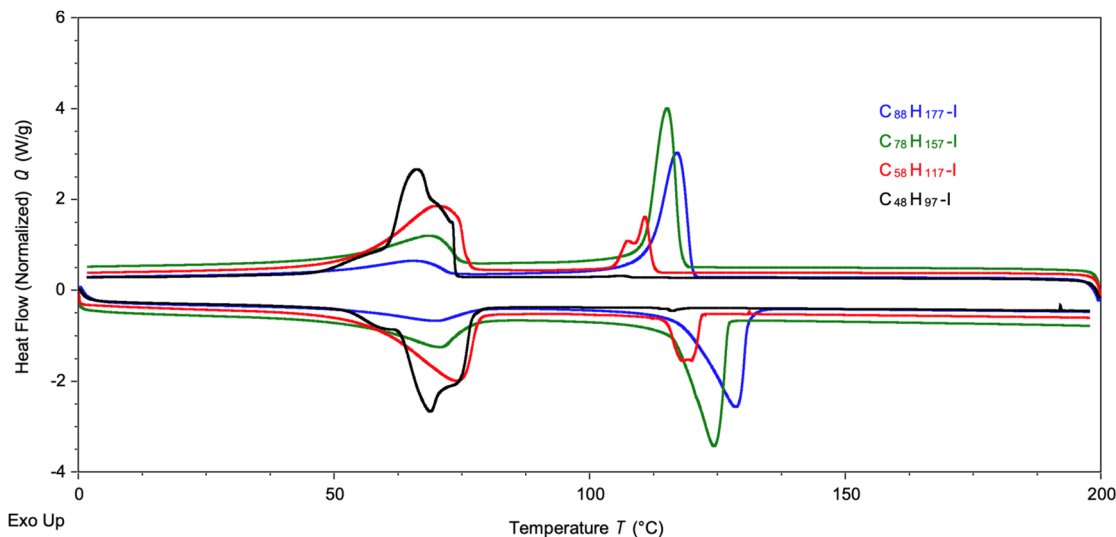


Fig. 4 DSC analysis of four PE-I samples of different chain length. Measurements shown were taken during the second heating cycle.

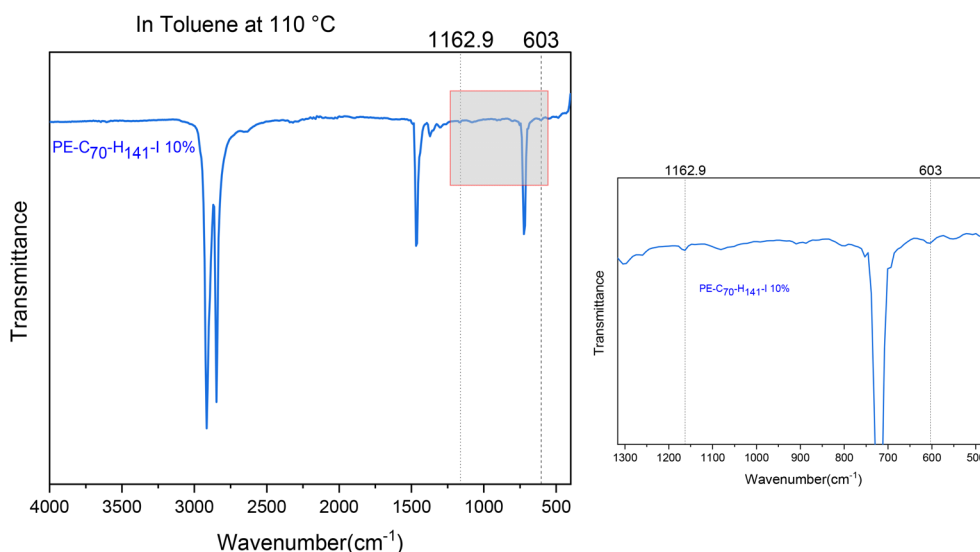


Fig. 5 FT-IR analysis of $C_{70}H_{141}I$ /LDPE polymer blend obtained via solution blending in toluene.

FIB-SEM and EDX analysis.^{82–84} The SEM image in Fig. 6 shows a magnification of the PE-I/LDPE polymer surface. A square hole of approximately $10 \times 10 \times 10 \mu\text{m}$ was cut by FIB micro machining using a gallium ion beam (see ESI for details[†]). EDX measurements were carried out at approximately $1 \mu\text{m}$ depth intervals up to $6 \mu\text{m}$ from the surface, as indicated in Fig. 6. Iodine was detected in all samples from its characteristic L_{α} signal at 3.937 keV , and there was no indication of a concentration gradient along this trajectory, indicating a random dispersion of PE-I, at least within $6 \mu\text{m}$ from the polymer surface.

In conclusion, we have shown that the CCG reaction of ZnEt_2 with ethylene, catalysed by the iron-based catalyst system $[(2,6\text{-diacetylpyridinebis}(2,6\text{-diisopropylanil}))\text{FeCl}_2]$ (**1**) and MAO gives access to ZnPE_2 , whereby the PE chain length can be controlled by the Zn/Fe ratio and the reaction time. The reaction of

ZnPE_2 with a variety of electrophiles leads to the formation of end-functionalised polyethylene PE-X. The selectivity for the formation of PE-OH appears to be limited to approximately 80%, probably due to the formation of zinc cluster $[\text{Zn}(\text{OR})\text{R}]_n$ intermediates. The reaction of ZnPE_2 with elemental sulfur results in the formation of polysulfides PE- S_k -PE. Polysulfides with $k > 3$ are thermally unstable and heating of PE- S_k -PE results in the elimination of sulfur and a lowering of k . The reaction of ZnPE_2 with iodine to generate PE-I is generally highly selective and is the preferred functionalisation method. Blends of PE-I and LDPE can be prepared by solution mixing or by melt blending through extrusion. These novel PE-I/LDPE polymer blends have been characterised by IR spectroscopy and DSC analysis. Surface analysis using SEM-EDX has indicated a uniform distribution of PE-I within $6 \mu\text{m}$ from the PE-I/LDPE surface.



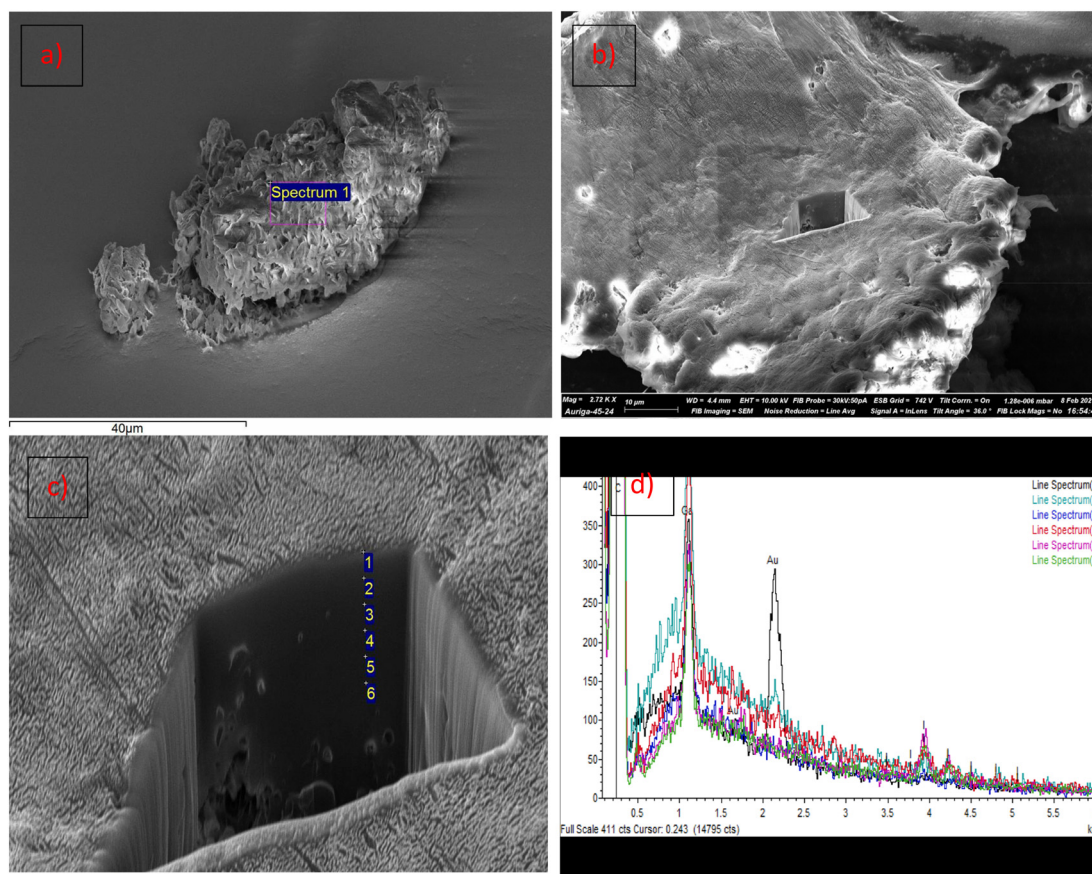


Fig. 6 (a) SEM image of PE-I/LDPE particle. (b) FIB-SEM image of PE-I/LDPE surface with square hole cut using FIB micro machining. (c) EDX analysis at $\sim 1 \mu\text{m}$ depth intervals. (d) EDX spectra taken at surface (spectrum 1) and at $\sim 1 \mu\text{m}$ depth intervals (SEM samples were Au-plated for conductivity).

Degradation studies of these novel PE-I/LDPE materials are currently underway and will be reported in due course.

Conflicts of interest

There are no conflicts of interest to declare.

Acknowledgements

We thank Polymateria Ltd for funding. Dr Mahmoud Ardakani is thanked for SEM and EDX measurements. We thank SABIC for a generous donation of LDPE (SABIC N0W2021) and AA is grateful for a scholarship from SABIC.

References

- 1 R. Geyer, J. R. Jambeck and K. L. Law, *Sci. Adv.*, 2017, **3**, 768–771.
- 2 M. Gahleitner, L. Resconi and P. Doshev, *MRS Bull.*, 2013, **38**, 229–233.
- 3 D. Jeremic, in *Ullmann's Encyclopedia of Industrial Chemistry*, 2014, pp. 1–42.
- 4 M. C. Baier, M. A. Zuideveld and S. Mecking, *Angew. Chem., Int. Ed.*, 2014, **53**, 9722–9744.
- 5 C. M. Plummer, L. Li and Y. Chen, *Poly. Chem.*, 2020, **11**, 6862–6872.
- 6 J. B. Williamson, W. L. Czaplyski, E. J. Alexanian and F. A. Leibfarth, *Angew. Chem., Int. Ed.*, 2018, **57**, 6261–6265.
- 7 N. M. Franssen, J. N. Reek and B. de Bruin, *Chem. Soc. Rev.*, 2013, **42**, 5809–5832.
- 8 P. D. Goring, C. Morton and P. Scott, *Dalton Trans.*, 2019, **48**, 3521–3530.
- 9 L. R. Sita, *Angew. Chem., Int. Ed.*, 2009, **48**, 2464–2472.
- 10 Y. J. Zhang, H. Y. Li, J. Y. Dong and Y. L. Hu, *Prog. Chem.*, 2014, **26**, 110–124.
- 11 A. Valente, A. Mortreux, M. Visseaux and P. Zinck, *Chem. Rev.*, 2013, **113**, 3836–3857.
- 12 G. J. P. Britovsek, S. A. Cohen, V. C. Gibson and M. van Meurs, *J. Am. Chem. Soc.*, 2004, **126**, 10701–10712.
- 13 I. Haas, W. P. Kretschmer and R. Kempe, *Organometallics*, 2011, **30**, 4854–4861.



- 14 R. Leino, H. J. G. Luttikhedde, P. Lehmus, C.-E. Wilén, R. Sjöholm, A. Lehtonen, V. J. Seppälä and J. H. Näsman, *Macromolecules*, 1997, **30**, 3477–3483.
- 15 L. Rocchigiani, V. Busico, A. Pastore and A. Macchioni, *Organometallics*, 2016, **35**, 1241–1250.
- 16 J. S. Rogers and G. C. Bazan, *Chem. Commun.*, 2000, 1209–1210.
- 17 K. Nomura, U. Tewasekson and Y. Takii, *Organometallics*, 2015, **34**, 3272–3281.
- 18 J. Obenauf, W. P. Kretschmer and R. Kempe, *Eur. J. Inorg. Chem.*, 2014, 1446–1453.
- 19 S. K. T. Pillai, W. P. Kretschmer, M. Trebbin, S. Förster and R. Kempe, *Chem. – Eur. J.*, 2012, **18**, 13974–13978.
- 20 E. C. Samsel and D. C. Eisenberg, Ethyl Corporation, EP0574854, 1993.
- 21 R. S. A. Meyer, J. S. Scholtyssek and G. A. Luinstra, *Macromol. Mater. Eng.*, 2015, **300**, 218–225.
- 22 C. J. Han, M. S. Lee, D.-J. Byun and S. Y. Kim, *Macromolecules*, 2002, **35**, 8923–8925.
- 23 W. P. Kretschmer, T. Bauer, B. Hessen and R. Kempe, *Dalton Trans.*, 2010, **39**, 6847–6852.
- 24 J.-F. Pelletier, A. Mortreux, X. Olonde and K. Bujadoux, *Angew. Chem., Int. Ed. Engl.*, 1996, **35**, 1854–1856.
- 25 T. Chenal, X. Olonde, J.-F. Pelletier, K. Bujadoux and A. Mortreux, *Polymer*, 2007, **48**, 1844–1856.
- 26 X. Olonde, A. Mortreux, F. Petit and K. Bujadoux, *J. Mol. Catal.*, 1993, **82**, 75–82.
- 27 R. Ribeiro, R. Ruivo, H. Nsiri, S. B. S. Norsic, F. D'Agosto, L. Perrin, C. Boisson, F. D'Agosto, L. Perrin and C. Boisson, *ACS Catal.*, 2016, **6**, 851–860.
- 28 G. J. P. Britovsek, S. A. Cohen, V. C. Gibson, P. J. Maddox and M. van Meurs, *Angew. Chem., Int. Ed.*, 2002, **41**, 489–491.
- 29 D. J. Arriola, E. M. Carnahan, P. D. Hustad, R. L. Kuhlman and T. T. Wenzel, *Science*, 2006, **312**, 714–719.
- 30 M. Van Meurs, G. J. P. Britovsek, V. C. Gibson and S. A. Cohen, *J. Am. Chem. Soc.*, 2005, **127**, 9913–9923.
- 31 A. Xiao, L. Wang, Q. Liu, H. Yu, J. Wang, J. Huo, Q. Tan, J. Ding, W. Ding and A. M. Amin, *Macromolecules*, 2009, **42**, 1834–1837.
- 32 W. Zhang, J. Wei and L. R. Sita, *Macromolecules*, 2008, **41**, 7829–7833.
- 33 O. H. Hashmi, M. Visseaux and Y. Champouret, *Polym. Chem.*, 2021, **12**, 4626–4631.
- 34 G. J. P. Britovsek, S. A. Cohen, V. C. Gibson, P. J. Maddox and M. van Meurs, *Angew. Chem., Int. Ed.*, 2002, **41**, 489–491.
- 35 R. Cariou and J. W. Shabaker, *ACS Catal.*, 2015, **5**, 4363–4367.
- 36 H. Kaneyoshi, Y. Inoue and K. Matyjaszewski, *Macromolecules*, 2005, **38**, 5425–5435.
- 37 F. He, P. Li, A. Wu, T. Xu, Z. Fu, L. Zhu and Z. Fan, *Polyolefins J.*, 2017, **4**, 191–200.
- 38 T. Li, W. J. Wang, R. Liu, W. H. Liang, G. F. Zhao, Z. Li, Q. Wu and F. M. Zhu, *Macromolecules*, 2009, **42**, 3804–3810.
- 39 P. Li, Z. Fu and Z. Fan, *J. Appl. Polym. Sci.*, 2015, **132**, 1–10.
- 40 Y. Zhao, X. Shi, H. Gao, L. Zhang, F. Zhu and Q. Wu, *J. Math. Chem.*, 2012, **22**, 5737–5745.
- 41 S. Rutkowski, A. Zych, M. Przybysz, M. Bouyahyi, P. Sowinski, R. Koevoets, J. Haponiuk, R. Graf, M. R. Hansen, L. Jasinska-Walc and R. Duchateau, *Macromolecules*, 2016, **50**, 107–122.
- 42 C. J. Han, M. S. Lee, D. J. Byun and S. Y. Kim, *Macromolecules*, 2002, **35**, 8923–8925.
- 43 J. Mazzolini, E. Espinosa, F. D'Agosto and C. Boisson, *Polym. Chem.*, 2010, **1**, 793–800.
- 44 T. Chenal, M. Drelon, B. Marsh, F. F. Silva, M. Visseaux and A. Mortreux, *Catal. Sci. Technol.*, 2020, **10**, 6809–6824.
- 45 T. Shiono, K. Yoshida and K. Soga, *Makromol. Chem., Rapid Commun.*, 1990, **11**, 169–175.
- 46 T. Shiono, K. Yoshida and K. Soga, *Stud. Surf. Sci. Catal.*, 1990, **56**, 285–299.
- 47 J. E. O. Mazzolini, I. Mokthari, R. Briquel, O. Boyron, F. E. Delolme, V. Monteil, D. Bertin, D. Gimes, F. D'Agosto and C. Boisson, *Macromolecules*, 2010, **43**, 7495–7503.
- 48 R. Briquel, J. Mazzolini, T. Le Bris, O. Boyron, F. Boisson, F. Delolme, F. D'Agosto, C. Boisson and R. Spitz, *Angew. Chem., Int. Ed.*, 2008, **47**, 9311–9313.
- 49 W. N. Ottou, S. Norsic, F. D'Agosto and C. Boisson, *Macromol. Rapid Commun.*, 2018, **39**, 1800154.
- 50 B. H. Staudt, J. Wagner and P. Vana, *Macromolecules*, 2018, **51**, 8469–8476.
- 51 P. L. Ross and M. V. Johnston, *J. Phys. Chem.*, 2002, **99**, 16507–16510.
- 52 P. L. Ross and M. V. Johnston, *J. Phys. Chem.*, 2002, **99**, 4078–4085.
- 53 P. J. Kropp and R. L. Adkins, *J. Am. Chem. Soc.*, 2002, **113**, 2709–2717.
- 54 G. Heimann, H.-J. Benkelberg, O. Böge and P. Warneck, *Int. J. Chem. Kinet.*, 2002, **34**, 126–138.
- 55 A. Ammala, S. Bateman, K. Dean, E. Petinakis, P. Sangwan, S. Wong, Q. Yuan, L. Yu, C. Patrick and K. H. Leong, *Prog. Polym. Sci.*, 2011, **36**, 1015–1049.
- 56 V. M. Litvinov, M. E. Ries, T. W. Baughman, A. Henke and P. P. Matloka, *Macromolecules*, 2013, **46**, 541–547.
- 57 G. J. P. Britovsek, M. Bruce, V. C. Gibson, B. S. Kimberley, P. J. Maddox, S. Mastroianni, S. J. McTavish, C. Redshaw, G. A. Solan, S. Strömberg, A. J. P. White and D. J. Williams, *J. Am. Chem. Soc.*, 1999, **121**, 8728–8740.
- 58 G. J. P. Britovsek, S. A. Cohen, V. C. Gibson and M. van Meurs, *J. Am. Chem. Soc.*, 2004, **126**, 10701–10712.
- 59 B. Nagel and W. Brüser, *Z. Anorg. Allg. Chem.*, 1980, **468**, 148–152.
- 60 C. T. Young, R. von Goetze, A. K. Tomov, F. Zaccaria and G. J. P. Britovsek, *Top. Catal.*, 2020, **63**, 294–318.
- 61 G. V. Schulz, *Makromol. Chem.*, 1950, **5**, 83–94.
- 62 S. Jana, R. J. F. Berger, R. Fröhlich, T. Pape and N. W. Mitzel, *Inorg. Chem.*, 2007, **46**, 4293–4297.
- 63 C. H. Bamford and D. M. Newitt, *J. Chem. Soc.*, 1946, 688.
- 64 W. Wang, L. P. Hou, T. Y. Zhang and C. C. Liu, *J. Polym. Res.*, 2018, **25**, 145.



- 65 J. Lewinski, W. Marciniak, J. Lipkowski and I. Justyniak, *J. Am. Chem. Soc.*, 2003, **125**, 12698–12699.
- 66 M. Kubisiak, K. Zelga, W. Bury, I. Justyniak, K. Budny-Godlewski, Z. Ochal and J. Lewinski, *Chem. Sci.*, 2015, **6**, 3102–3108.
- 67 L. Makolski, V. Szejko, K. Zelga, A. Tulewicz, P. Bernatowicz, I. Justyniak and J. Lewinski, *Chemistry*, 2021, **27**, 5666–5674.
- 68 J. Maury, L. Feray, S. Bazin, J. L. Clement, S. R. A. Marque, D. Siri and M. P. Bertrand, *Chem. – Eur. J.*, 2011, **17**, 1586–1595.
- 69 T. Hasell, D. J. Parker, H. A. Jones, T. McAllister and S. M. Howdle, *Chem. Commun.*, 2016, **52**, 5383–5386.
- 70 Y. Zhang, R. S. Glass, K. Char and J. Pyun, *Polym. Chem.*, 2019, **10**, 4078–4105.
- 71 J. J. Griebel, R. S. Glass, K. Char and J. Pyun, *Prog. Polym. Sci.*, 2016, **58**, 90–125.
- 72 J. F. Boscato, J. M. Catala, E. Franta and J. Brossas, *Tetrahedron Lett.*, 1980, **21**, 1519–1520.
- 73 D. Zeng, M. J. Hampden-Smith and E. N. Duesler, *Inorg. Chem.*, 1994, **33**, 5376–5377.
- 74 M. D. Nyman, M. J. Hampden-Smith and E. N. Duesler, *Inorg. Chem.*, 1996, **35**, 802–803.
- 75 D. Lin-Vien, N. Colthup, W. Fateley and J. G. Graselli, *Infrared and Raman Characteristic Frequencies of Organic Molecules*, Academic Press, San Diego, 1991.
- 76 P. D. Clark and C. O. Oriakhi, *Energy Fuels*, 1992, **6**, 474–477.
- 77 M. F. Bolotnikov and Y. A. Neruchev, *Russ. J. Phys. Chem. A*, 2007, **81**, 1198–1202.
- 78 G. R. Somayajulu, *Int. J. Thermophys.*, 1990, **11**, 555–572.
- 79 J. Visjager, T. A. Tervoort and P. Smith, *Polymer*, 1999, **40**, 4533–4542.
- 80 E. P. Gilbert, *Phys. Chem. Chem. Phys.*, 1999, **1**, 1517–1529.
- 81 S. L. Wong, N. Ngadi and T. A. T. Abdullah, *Appl. Mech. Mater.*, 2014, **695**, 170–173.
- 82 W. Brostow, B. P. Gorman and O. Olea-Mejia, *Mater. Lett.*, 2007, **61**, 1333–1336.
- 83 M. Kato, T. Ito, Y. Aoyama, K. Sawa, T. Kaneko, N. Kawase and H. Jinnai, *J. Polym. Sci., Part B: Polym. Lett.*, 2007, **45**, 677–683.
- 84 E. Beach, M. Keefe, W. Heeschen and D. Rothe, *Polymer*, 2005, **46**, 11195–11197.

